



Improving the soft X-ray reflectivity of Cr/Ti multilayers by co-deposition of B₄C

Jingtao Zhu,^{a*} Jiayi Zhang,^a Haochuan Li,^a Yuchun Tu,^{a,b} Jinwen Chen,^a Hongchang Wang,^c Sarnjeet S. Dhesi,^c Mingqi Cui,^d Jie Zhu^a and Philippe Jonnard^b

^aMOE Key Laboratory of Advanced Micro-structured Materials, Institute of Precision Optical Engineering, School of Physics Science and Engineering, Tongji University, Shanghai 200092, People's Republic of China, ^bSorbonne Université, Faculté des Sciences et Ingénierie, UMR CNRS, Laboratoire de Chimie Physique – Matière et Rayonnement, 4 Place Jussieu, F-75252 Paris Cedex 05, France, ^cDiamond Light Source, Harwell Science and Innovation Campus, Didcot, Oxfordshire OX11 0DE, United Kingdom, and ^dBeijing Synchrotron Radiation Facility, Institute of High Energy Physics, Chinese Academic of Science, Beijing 200092, People's Republic of China. *Correspondence e-mail: jtzhu@tongji.edu.cn

Received 13 January 2020

Accepted 27 August 2020

Edited by U. Jeng, NSRRC, Taiwan

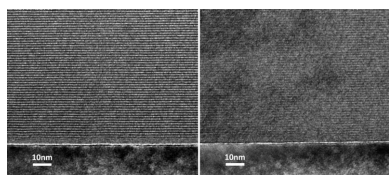
Keywords: synchrotron radiation; multilayer; interface; Cr/Ti.

The 'water window', covering 2.4–4.4 nm, is an important wavelength range particularly essential to biology research. Cr/Ti multilayers are one of the promising reflecting elements in this region because the near-normal-incidence reflectivity is theoretically as high as 64% at 2.73 nm. However, due to multilayer imperfections, the reported reflectivity is lower than 3% for near-normal incidence. Here, B and C were intentionally incorporated into ultra-thin Cr/Ti soft X-ray multilayers by co-deposition of B₄C at the interfaces. The effect on the multilayer structure and composition has been investigated using X-ray reflectometry, X-ray photoelectron spectroscopy, and cross-section electron microscopy. It is shown that B and C are mainly bonded to Ti sites, forming a nonstoichiometric TiB_xC_y composition, which hinders the interface diffusion, suppresses the crystallization of the Cr/Ti multilayer and dramatically improves the interface quality of Cr/TiB_xC_y multilayers. As a result, the near-normal-incidence reflectivity of soft X-rays increases from 4.48% to 15.75% at a wavelength of 2.73 nm.

1. Introduction

Multilayer coatings for the soft X-ray region have drawn a great deal of attention due to their vital importance in high-resolution microscopes, deep-space telescopes, and soft X-ray polarimetry (Artyukov *et al.*, 2009; Windt *et al.*, 2004; Kitamoto *et al.*, 2010). In these applications, reflectivity is one of the most critical parameters of a multilayer. Cr/Ti multilayers are one of the suitable candidates in the 'water window' wavelength range (2.4–4.4 nm) because the theoretical near-normal-incidence reflectivity is as high as 64% at wavelengths just above the Ti 2*p* edge (2.73 nm). However, the reported reflectivity of real Cr/Ti multilayers at near-incidence angles is lower than 3% (Ghafoor *et al.*, 2006). The large disparity between the theoretical and measured reflectivity is caused by several physical limitations, among which the most important are interfacial imperfections, especially for the ultra-short periods ($\Lambda \simeq 1.4$ nm) used.

In recent years there has been a huge effort to develop techniques that can reduce the interface width of multilayers. One recent attempt involved the intentional incorporation of light-element impurities such as N into multilayers. It has been shown that the incorporation of N in Cr/Sc (Ghafoor *et al.*, 2008) or B₄C/La (Tsarfati *et al.*, 2010) multilayers can form nonstoichiometric nitride multilayers with reduced interdiffusion or reaction between the constituent layers and leads



to major improvement in soft X-ray reflectivity. Another scheme is the introduction of B_4C , which has been effective in Cr/Sc (Ghafoor *et al.*, 2017) and Cr/V (Huang *et al.*, 2016) systems. For Cr/Ti multilayers, B or C is a better choice than N because of stronger absorption of N in the applicable wavelength range of Cr/Ti multilayers, which is slightly lower than the N K -edge (3.02 nm). In this work, we intentionally incorporated B and C and investigated the effects of B and C impurities on the microstructure and optical performance of the multilayers.

2. Fabrication

Cr/Ti multilayers were deposited by DC magnetron sputtering with B and C impurities incorporated by the deposition of ultra-thin B_4C at the interfaces of Cr/Ti multilayers. All the multilayers were deposited onto a natively oxidized Si (001) wafer with roughness of 0.3 nm. The pressure of the residual gas before deposition was 5.0×10^{-5} Pa and that of Ar sputtering gas was 0.13 Pa with a purity of 99.999%. Sub-nanometre thin layers were obtained by optimizing target–substrate distances and magnetron power. Target–substrate distances were all 8 cm. The magnetron power of B_4C , Cr and Ti were 40 W, 20 W and 40 W, respectively. Experiment details can be found in the PhD thesis by Yunchun Tu (Tu, 2015).

3. Characterization for the interfaces of Cr/Ti multilayers

Firstly, we studied the effect of different amounts and interfaces of the incorporated B_4C . We deposited a series of Cr/Ti multilayers, which can be divided into four groups. All the multilayers were designed with period number $N = 50$. B_4C was incorporated at both Cr-on-Ti and Ti-on-Cr interfaces for the first group, at only Cr-on-Ti interfaces for the second group, and at only Ti-on-Cr interfaces for the third group. The multilayers in those three groups were deposited with the same thicknesses of Cr layers and Ti layers ($d_{Ti} = d_{Cr} = 0.7$ nm). Each of those three groups consisted of six multilayers with different amounts of B_4C , where one multilayer had no B_4C , and the nominal amounts (in thickness) of B_4C for the other five multilayers were 0.08, 0.13, 0.18, 0.22 and 0.27 nm, respectively. For comparison, the last group contained four pure Cr/Ti multilayers without B_4C . The period thicknesses of the four multilayers ranged from 1.4 nm to 1.7 nm and their thickness ratio ($\Gamma = d_{Cr}/\Lambda$) was ~ 0.5 .

All the multilayers were characterized by low-angle X-ray reflectometry (XRR). Measurements were performed on a Bede D1 diffractometer with a Cu X-ray source ($\lambda = 0.154$ nm). Only the first-order Bragg peak could be observed for each multilayer because of the ultra-short period. We present the peak reflectivity as a function of the grazing-incident angle in Fig. 1, where thicker multilayers correspond to the smaller grazing angle (left side). It can be seen from the figure that incorporating B_4C at either or both interfaces leads to higher reflectivity, namely improved multilayer quality. In particular, it is better to incorporate B_4C at the Cr-on-Ti

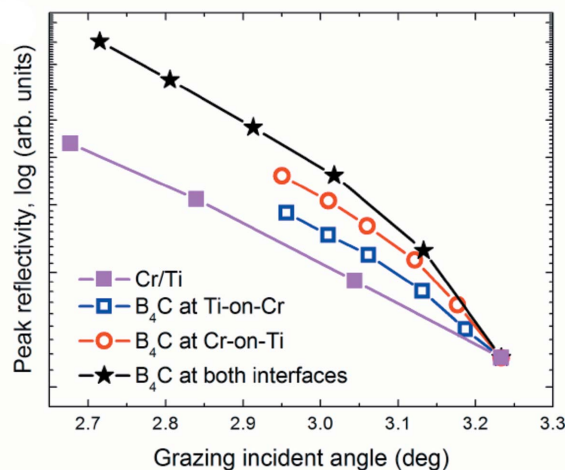


Figure 1 Peak reflectivity versus peak angle of the first-order Bragg peaks in the XRR curves of the Cr/Ti multilayers. Symbols represent the data and solid lines are only a guide for the eye.

interfaces than at the Ti-on-Cr interfaces, and incorporating B_4C at both types of interfaces proved to be the best of all. A thickness of 0.13 nm B_4C was chosen because the fitted roughness was the lowest.

In order to study the interface stoichiometry, we performed X-ray photoelectron spectroscopy (XPS) measurements on two samples. One had no B_4C incorporated and the other had 0.13 nm-thick B_4C at both interfaces. The measurements were performed on a Thermo Scientific K-Alpha system with an Al $K\alpha$ source. The binding energy scale was calibrated from hydrocarbon contamination using the C 1s peak at 285.0 eV. Core peaks were analyzed using a nonlinear Shirley-type background. The peak positions and areas were optimized by a weighted least-squares fitting method using 70% Gaussian/30% Lorentzian line shapes. Atomic concentrations were calculated on the basis of Scofield's relative sensitivity factors. To eliminate the contamination of the multilayer such as the oxidation at the surface, the XPS spectra were recorded after ~ 10 nm of material near the surface was removed by Ar⁺ etching. Considering the ultra-short period, it is safe to regard the recorded spectra as averaged results over the whole multilayer period. It should be noted that, for some material combinations, the chemical interaction of materials in the multilayer may change after energetic Ar⁺ ion bombardment. More specific investigations on such an issue could be performed by further research. The B 1s and C 1s spectra of the multilayer with B_4C are shown in Fig. 2 along with the spectra of a B_4C monolayer reference sample which was deposited and measured by the same method as described above. The B 1s spectrum of the monolayer consists of two peaks at 188.4 eV, characteristic of B–B or B–C bonds from B atoms in the B_{12} icosahedra, and 190.6 eV, characteristic of B–C bonds from B atoms in the C–B–C chain. The B 1s spectrum of the Cr/Ti multilayer is dominated by a peak at 187.4 eV which is attributed to TiB_2 (187.5 eV) (Mavel *et al.*, 1973) rather than CrB_2 (188.0 eV) (Mavel *et al.*, 1973). The C 1s spectrum of the monolayer consists of two peaks at

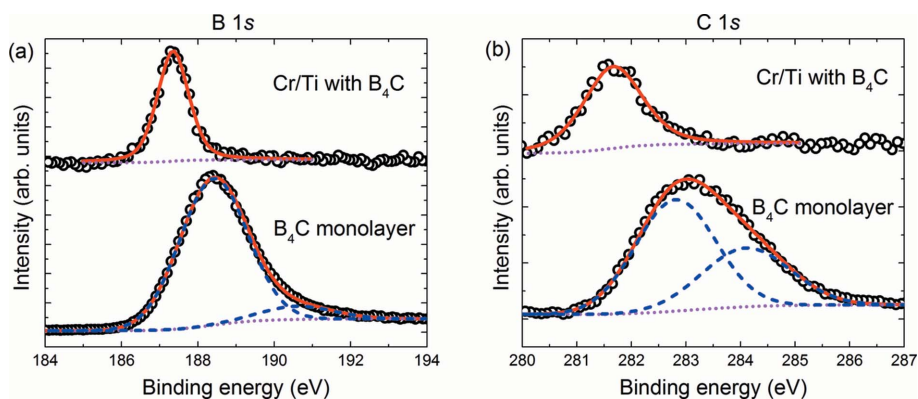


Figure 2
 (a) B 1s and (b) C 1s XPS spectra of the B₄C monolayer and Cr/Ti multilayer with B₄C. Open symbols represent the measured data, solid lines the fitted spectra, short dashed lines the background, and long dashed lines the peaks used in the fitting if more than one peak is involved.

282.8 eV, characteristic of B–C bonds in the icosahedra, and 284.1 eV, characteristic of B–C bonds in the C–B–C chain. The C 1s spectra of the Cr/Ti multilayer is dominated by a peak at 281.9 eV which is attributed to TiC (281.7 eV) (Galuska *et al.*, 1988) rather than Cr₃C₂ (282.9 eV) (Goretzki *et al.*, 1989). For the pure Cr/Ti multilayer, the atomic concentrations of Cr, Ti, and O are 58.9%, 27.8%, and 13.4%, respectively. For the Cr/Ti multilayer with B₄C, the atomic concentrations of Cr, Ti, B, C, and O are 47.8%, 22.9%, 17.1%, 4.4%, and 7.9%, respectively. There are two reasons why there is less oxygen in the Cr/B₄C/Ti/B₄C multilayer: firstly, B₄C can hinder the diffusion of oxygen to inner layers; secondly, with the co-deposition of B₄C, imperfections of the grain boundary can be decreased and thus there are fewer ways for oxygen to diffuse into inner layers. According to the calculated results, different concentrations of oxygen will not influence the reflectivity.

Encouraged by the preliminary results, we deposited two Cr/Ti multilayers, one without B₄C and the other with 0.13 nm-thick B₄C at both interfaces. The periodic number is $N = 600$ and the designed period thickness is $\Lambda = 1.38$ nm, which can work as a high-reflection mirror for wavelength $\lambda = 2.73$ nm (photon energy $E = 453.5$ eV). Fig. 3 shows cross-section transmission electron microscopy (TEM) images for the two samples measured using an FEI microscope (Tecnai G2 F20). The multilayer with B₄C shows much better contrast

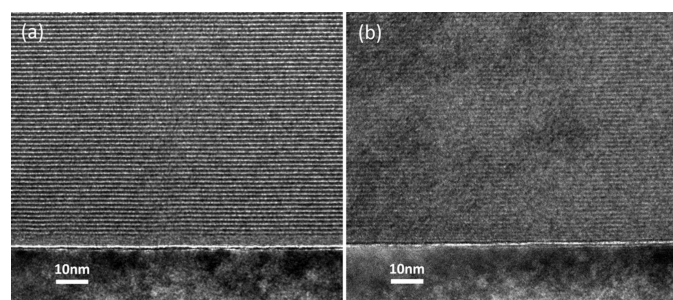


Figure 3
 Cross-section TEM graphs of Cr/Ti multilayers (a) with and (b) without B₄C.

between Cr layers and Ti layers although the flatness is similar. Fig. 4 presents the selected area diffraction (SAD) results of the Cr/Ti multilayer with and without B₄C. The diffraction ring and spots weakened after co-deposition of B₄C. The crystallization in the Cr/Ti multilayer has been suppressed. These results confirm that the TiB_xC_y formation prevents diffusion of Cr.

4. Reflectivity measurements at Diamond Light Source

The soft X-ray reflectivity measurements were performed using a high-precision polarimeter on beamline I06 at Diamond Light Source, UK (Wang *et al.*, 2011). The Cr filter was selected to suppress the high harmonic contamination from the collimated plane-grating monochromator, and linear horizontal polarization synchrotron radiation with energy $E = 453.5$ eV was used in the measurements. The reflectivity is plotted in Fig. 5 as a function of the incidence angle. The reflectivity of

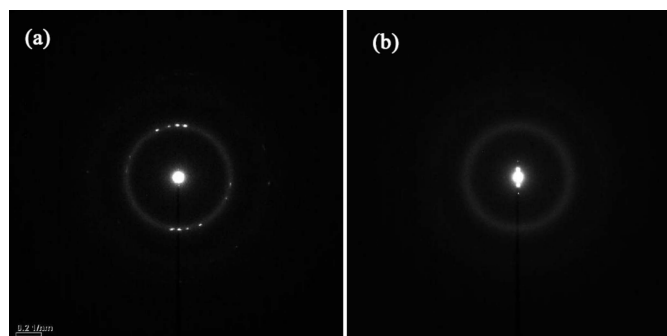


Figure 4
 SAD (selected area diffraction) results of (a) Cr/Ti multilayer and (b) Cr/B₄C/Ti/B₄C multilayer.

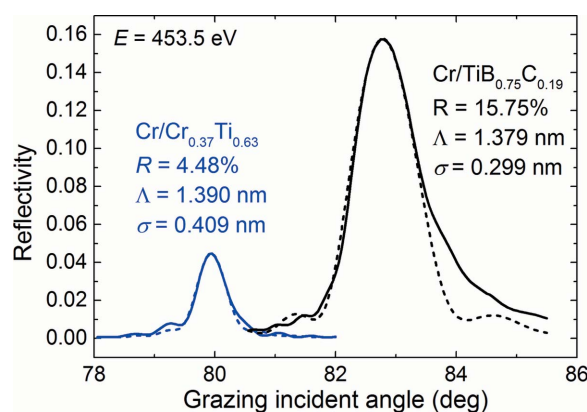


Figure 5
 Soft X-ray reflectivity of the Cr/Ti multilayers with and without B₄C. Solid lines represent the measured data and dashed lines show the calculated reflectivities.

the pure Cr/Ti multilayer is $R = 4.48\%$ (at 79.95°) and the interface width is determined to be $\sigma = 0.409$ nm by simulation using the *IMD* code (Windt, 1998). The reflectivity of the Cr/Ti multilayer with B_4C is $R = 15.75\%$ (at 82.75°) and the interface width is determined to be $\sigma = 0.299$ nm. The required optical constants were generated following the online method (Berkeley Center for X-ray Optics, <http://www-cxro.lbl.gov>). The large improvement in the reflectivity is due to the reduced diffusion between the Cr and Ti layer and the suppression of crystallization.

5. Summary

In this paper, we have presented pure Cr/Ti multilayers with ultra-short period ($\Lambda \simeq 1.4$ nm). We intentionally incorporated B and C into Cr/Ti multilayers by depositing ultra-thin B_4C at the interfaces. We found that incorporating 0.13 nm-thick B_4C at both interfaces dramatically influences the structure and composition of the Cr/Ti multilayers. B and C incorporated during deposition is mainly bonded to Ti. The formation of nonstoichiometric Ti compound hinders the diffusion and improves the interface quality of the multilayer. The crystallization is also suppressed after introduction of B_4C . As a result, Cr/ B_4C /Ti/ B_4C multilayers (with periodic number $N = 600$) exhibit $\sim 250\%$ higher near-normal-incidence soft X-ray reflectivity (absolute reflectivity $R = 15.75\%$) than pure Cr/Ti multilayers.

Acknowledgements

The authors acknowledge Francesco Maccherozzi for the support during the reflectivity measurements, Kawal Sawhney for helpful discussion and Yuchun Tu for the experimental suggestions.

Funding information

The following funding is acknowledged: Natural National Science Foundation of China (grant No. 11875204); Natural

National Science Foundation of China (grant No. 11775295); Natural National Science Foundation of China (grant No. 11575127); Fundamental Research Funds for the Central Universities (grant No. 22120180070); the Funds from Youth Innovation Promotion Association.

References

- Artyukov, I., Bugayev, Y., Devizenko, O., Gullikson, E., Kondratenko, V. & Vinogradov, A. (2009). *Opt. Lett.* **34**, 2930–2932.
- Galuska, A., Uht, J. & Marquez, N. (1988). *J. Vac. Sci. Technol. A*, **6**, 110–122.
- Ghafoor, N., Eriksson, F., Aquila, A., Gullikson, E., Schäfers, F., Greczynski, G. & Birch, J. (2017). *Opt. Express*, **25**, 18274–18287.
- Ghafoor, N., Eriksson, F., Gullikson, E., Hultman, L. & Birch, J. (2008). *Appl. Phys. Lett.* **92**, 091913.
- Ghafoor, N., Persson, P. O., Birch, J., Eriksson, F. & Schäfers, F. (2006). *Appl. Opt.* **45**, 137–143.
- Goretzki, H., Rosenstiel, P. v. & Mandziej, S. (1989). *Z. Anal. Chem.* **333**, 451–452.
- Huang, Q., Fei, J., Liu, Y., Li, P., Wen, M., Xie, C., Jonnard, P., Giglia, A., Zhang, Z., Wang, K. & Wang, Z. (2016). *Opt. Lett.* **41**, 701–704.
- Kitamoto, S., Murakami, H., Shishido, Y., Gotoh, N., Shibata, T., Saito, K., Watanabe, T., Kanai, J., Takenaka, E., Nagasaki, K., Yoshida, M., Takei, D. & Morii, M. (2010). *Rev. Sci. Instrum.* **81**, 023105.
- Mavel, G., Escard, J., Costa, P. & Castaing, J. (1973). *Surf. Sci.* **35**, 109–116.
- Tsarfaty, T., van de Kruijs, R. W. E., Zoethout, E., Louis, E. & Bijkerk, F. (2010). *Thin Solid Films*, **518**, 7249–7252.
- Tu, Y. (2015). PhD thesis, Université Pierre et Marie Curie-Paris VI, Paris, France (<https://tel.archives-ouvertes.fr/tel-01134315v2>).
- Wang, H., Dhési, S., Maccherozzi, F., Cavill, S., Shepherd, E., Yuan, F., Deshmukh, R., Scott, S., van der Laan, G. & Sawhney, K. (2011). *Rev. Sci. Instrum.* **82**, 123301.
- Windt, D. L. (1998). *Comput. Phys.* **12**, 360–370.
- Windt, D. L., Donguy, S., Seely, J. F., Kjørnattawanich, B., Gullikson, E. M., Walton, C., Golub, L. & DeLuca, E. (2004). *Optics for EUV, X-ray, and Gamma-Ray Astronomy*, pp. 1–11. International Society for Optics and Photonics.